

IN SITU THERMAL MAGNETIC INVESTIGATION
OF γ - $\text{MnC}_2\text{O}_4 \cdot 2\text{H}_2\text{O}$ DECOMPOSITION

Boriana Donkova, Dimitar Mehandjiev*

(Submitted by Academician P. Bonchev on February 14, 2013)

Abstract

Prismatic, well-shaped crystals of orthorhombic γ - $\text{MnC}_2\text{O}_4 \cdot 2\text{H}_2\text{O}$ were obtained by phase transformation of the initially synthesized $\text{MnC}_2\text{O}_4 \cdot 3\text{H}_2\text{O}$ and characterized by XRD, SEM, DTA and DTG analyses. The results from in situ thermal magnetic measurements were compared with those of the monoclinic α - $\text{MnC}_2\text{O}_4 \cdot 2\text{H}_2\text{O}$ and orthorhombic $\text{MnC}_2\text{O}_4 \cdot 3\text{H}_2\text{O}$. At γ - $\text{MnC}_2\text{O}_4 \cdot 2\text{H}_2\text{O}$ the magnetic interaction between Mn(II) ions is most intensive and before the beginning of decomposition it changes twice from antiferro- to ferromagnetic. For all crystal forms of the manganese(II) oxalate, the oxidative decomposition leads not only to Mn(III) but also to Mn(IV). However, the oxidation ability of Mn(II) is highest in monoclinic α - $\text{MnC}_2\text{O}_4 \cdot 2\text{H}_2\text{O}$ and similar for both orthorhombic crystal forms.

Key words: decomposition, magnetic measurements, manganese (II) oxalate

Introduction. In a system containing $\text{Mn}^{2+}-\text{C}_2\text{O}_4^{2-}-\text{H}_2\text{O}$, three crystal forms could be obtained depending on the synthesis conditions – monoclinic α - $\text{MnC}_2\text{O}_4 \cdot 2\text{H}_2\text{O}$ (SG C2/c) [1], orthorhombic γ - $\text{MnC}_2\text{O}_4 \cdot 2\text{H}_2\text{O}$ (P2₁2₁2₁) [2] and orthorhombic trihydrate $\text{MnC}_2\text{O}_4 \cdot 3\text{H}_2\text{O}$ (Pcca) [3]. In our previous paper [4] on the thermal-magnetic investigation of decomposition mechanism of α - $\text{MnC}_2\text{O}_4 \cdot 2\text{H}_2\text{O}$ and $\text{MnC}_2\text{O}_4 \cdot 3\text{H}_2\text{O}$, the conclusion was that during calcination in air the oxidation of Mn(II) proceeds not only to Mn(III) but also to Mn(IV), which further passes to lower oxidation states. It was shown that difference in the crystal lattice is responsible for both different thermal behaviour of the samples

The authors acknowledge the financial support of project UNION (DO-02-82/2008).

and the different extent of the Mn(II) oxidation, thus leading to different oxide products at the same annealing temperature. The aim of the present paper is to report the preliminary data about the thermal decomposition mechanism of the third form – γ - $\text{MnC}_2\text{O}_4 \cdot 2\text{H}_2\text{O}$, using again in situ measurements of its magnetic properties. This method allows direct determination of the oxidation state of manganese ions and its coordination during the decomposition process. As far as we know, there is only one report, concerning the kinetics of γ - $\text{MnC}_2\text{O}_4 \cdot 2\text{H}_2\text{O}$ decomposition and using XRD and SEM methods for characterization of the products obtained [5].

Experimental part. Orthorhombic pinkish γ - $\text{MnC}_2\text{O}_4 \cdot 2\text{H}_2\text{O}$ is the thermodynamically most stable form in the system $\text{Mn}^{2+} - \text{C}_2\text{O}_4^{2-} - \text{H}_2\text{O}$, therefore it was obtained by phase transformation of the initially synthesized $\text{MnC}_2\text{O}_4 \cdot 3\text{H}_2\text{O}$ after prolonged residence time in the supernatant liquor. The procedure for $\text{MnC}_2\text{O}_4 \cdot 3\text{H}_2\text{O}$ precipitation was described by us in [4]. The obtained pink precipitate was left in contact with the mother liquid and an optical microscopy observation was conducted periodically to monitor the phase transitions. After five months, the resulting pinkish product was filtrated, washed several times and dried in air.

The XRD analysis of the sample was carried out with a D500 Siemens powder diffractometer using Cu K radiation. The thermal investigation was performed in a synthetic air atmosphere (20 ml/min) with sample mass of 2 mg at a heating rate of $10^\circ\text{C}/\text{min}$ in the range of 25 – 500°C using LABSYSTEM EVO instrument (SETARAM, France). The measurements of magnetic susceptibility were carried out in the range of 25 – 300°C with a Faraday type magnetic balance in accordance with the method described in [4, 6]. The respective weight loss (WL) was also determined. The effective magnetic moments of manganese ions (μ_{eff}) were calculated on the basis of the Curie–Weiss law as $\mu_{\text{eff}} = 2.828 [\chi_{\text{M}}(\text{T}-\theta)]^{1/2}$, where χ_{M} is the molar magnetic susceptibility; T is the absolute temperature in K; θ is the Weiss constant in K. The validity of the Curie–Weiss law was checked by magnetic measurement in the range of -95°C to $+20^\circ\text{C}$.

Results and discussion. The X-ray pattern of the obtained product is represented in Fig. 1 and confirms the complete transformation of initial trihydrate in γ - $\text{MnC}_2\text{O}_4 \cdot 2\text{H}_2\text{O}$ (JPCDS 32-0647). The strongest reflections of $\text{MnC}_2\text{O}_4 \cdot 3\text{H}_2\text{O}$ and α - $\text{MnC}_2\text{O}_4 \cdot 2\text{H}_2\text{O}$ are not observed. The sharp and narrow diffraction peaks indicate the good crystallinity of the sample. This statement is confirmed by the SEM images (Fig. 2). Well-shaped tetrahedral prisms are observed (in some cases with pyramidal termination) and the shape is very different both from the smooth needle-like crystals of the trihydrate and rose-like agglomerates of monoclinic α - $\text{MnC}_2\text{O}_4 \cdot 2\text{H}_2\text{O}$.

The DTA and DTG curves are shown in Fig. 3. According to the derivative $d(\text{TG})/dT$ curve, which expresses more clearly the changes occurring with the specimen, dehydration occurs in the range of 120 – 180°C . The water liberation

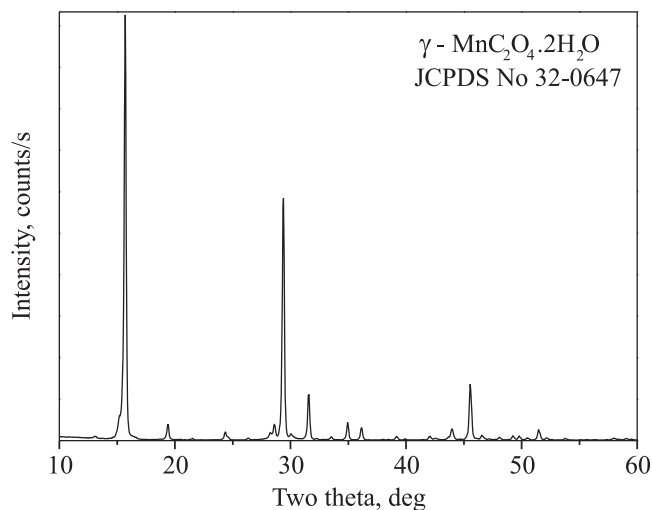


Fig. 1. XRD pattern of the orthorhombic γ - $\text{MnC}_2\text{O}_4 \cdot 2\text{H}_2\text{O}$

proceeds in one step with peak position of heat flow at 155°C . For comparison the dehydration of α - $\text{MnC}_2\text{O}_4 \cdot 2\text{H}_2\text{O}$ proceeds in the same way, but at higher temperature, while that of $\text{MnC}_2\text{O}_4 \cdot 3\text{H}_2\text{O}$ is in three steps. The experimental weight loss (WL) at the end of the steep slope of TG curve is 19%, which slowly increases to the calculated value of 20% at the end of the smooth section. According to DTA and DTG curves, the intensive decomposition takes place in the interval of 262 – 362°C (peak at 317°C). However, the evolution of CO_2 (Fig. 3) starts at a lower temperature, suggesting that decomposition has already begun. This fact fully supports the statements that in air medium the oxidation to Mn(III) takes place just before decomposition and catalyzes the latter [7, 8]. Due to the low sam-

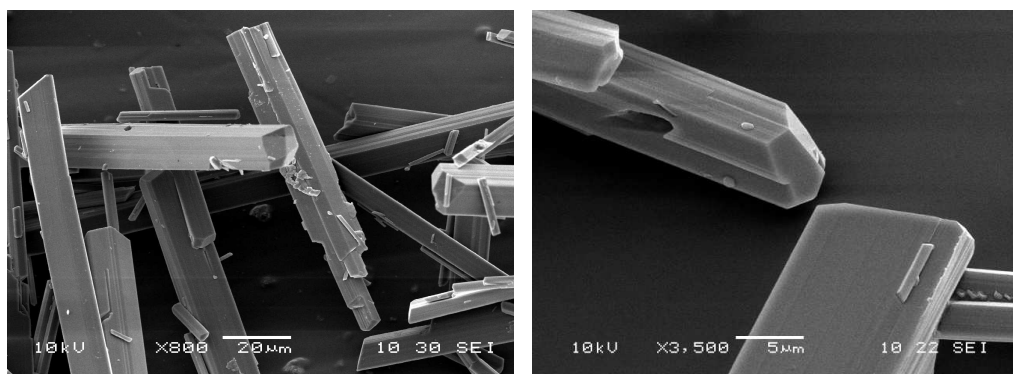


Fig. 2. Scanning electron micrographs of γ - $\text{MnC}_2\text{O}_4 \cdot 2\text{H}_2\text{O}$

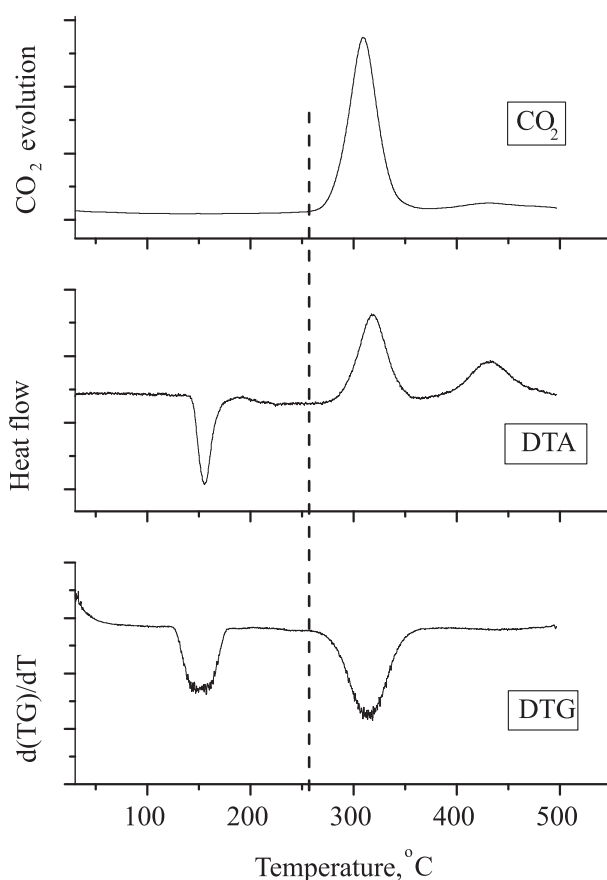


Fig. 3. DTA, DTG and CO₂ evolution curves. (The dash line compares the initial temperatures of the observed changes.)

ple weight, the process of oxidative decomposition can be clearly distinguished from the next secondary process (peak at 432 °C), accompanied by evolution of additional CO₂ and absence of noticeable changes in the TG and DTG curves. Most probably, Mnⁿ⁺ and Mn^{m+} available in the system catalyze the oxidation of CO to CO₂ [8], but to clarify the nature of this peak additional studies are necessary to be performed.

Figure 4a, b represents the temperature dependence of the specific magnetic susceptibility (χ_s) of γ -MnC₂O₄·2H₂O and the change of the sample weight in the range of 25–300 °C. The decrease of χ_s with the increase of temperature shows that the sample displays paramagnetic properties as the other two forms – α -MnC₂O₄·2H₂O and MnC₂O₄·3H₂O. Local deviations from the trend of the curve are observed due to the changes in the magnetic properties and weight of the sample during dehydration and decomposition processes. An intensive dehy-

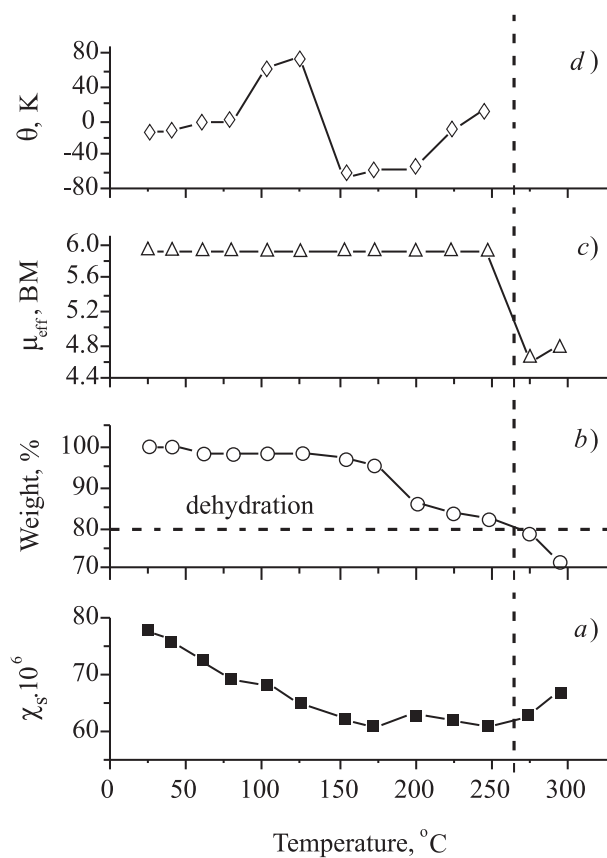


Fig. 4. Temperature dependence of: a) specific magnetic susceptibility – χ_s ; b) weight; c) effective magnetic moment – μ_{eff} ; d) Weiss constant – θ during in situ magnetic measurements. (Intersection of the dash lines shows the temperature at the end of the dehydration process.)

dration is carried out in the range of ~ 150 to $\sim 265^\circ\text{C}$ (Fig. 4b), after that the decomposition takes place. The liberated H_2O is diamagnetic and retards the decrease in the susceptibility with temperature. Therefore, retention and even a small local increase of the χ_s , can be seen in Fig. 4a. The beginning of decomposition above 265°C leads to additional increase of χ_s . This trend is likely to be determined by the formation of new phases and especially by the manganese oxidation state.

To determine the oxidation state of manganese and its changes during decomposition, the effective magnetic moments (μ_{eff}) were calculated. The value of the μ_{eff} depends on the oxidation state of manganese, its coordination, and the strength of the crystal field [9, 10]. In the case of the oxalate ions, the octahedral

crystal field of an intermediate strength should be expected and the theoretical values of μ_{eff} for the various oxidation states are 5.92 BM for Mn(II), 4.70 BM for Mn(III), and 3.44 BM for Mn(IV) [9]. For $\gamma\text{-MnC}_2\text{O}_4\cdot 2\text{H}_2\text{O}$ the calculated μ_{eff} value at room temperature is 5.92 BM, which means that manganese is in the (+2) oxidation state and high spin configuration ($S = 5/2$). The calculated Weiss constant is $\theta = -15$ K and its negative value indicates an antiferromagnetic interaction between Mn ions in $\gamma\text{-MnC}_2\text{O}_4\cdot 2\text{H}_2\text{O}$ like the other two crystal forms.

Temperature dependence of the calculated μ_{eff} is shown in Fig. 4c. Since the oxidation state of Mn(II) is being preserved during the entire dehydration process, which ends at 265 °C, the magnetic moment should not be changed. However, due to the structural relaxation, a change in the Weiss constant (θ) is expected at this stage because the sign and value of θ are determined by the exchange integral and the number of neighbours which the respective ions are interacting with [9, 10].

Figure 4d shows the temperature dependence of the Weiss constant in the range of 25–265 °C, calculated at $\mu_{\text{eff}} = 5.92$ BM. From the beginning of the increase in temperature, the θ value becomes higher and a change in the sign is observed even before the weight change of the sample. In the shown interval, the negative sign of θ changes twice – evidence for change in the interaction between Mn(II) from antiferro- to ferromagnetic. Although the accuracy in the θ calculation at these conditions is not so high, providing experiments on the same magnetic balance allows us to compare the behaviour of the three crystal forms during the dehydration process. The initial values of Weiss constant are the same: $\theta = -14$ K for $\alpha\text{-MnC}_2\text{O}_4\cdot 2\text{H}_2\text{O}$, $\theta = -16$ K for $\text{MnC}_2\text{O}_4\cdot 3\text{H}_2\text{O}$ and $\theta = -15$ for $\gamma\text{-MnC}_2\text{O}_4\cdot 2\text{H}_2\text{O}$. In the case of $\alpha\text{-MnC}_2\text{O}_4\cdot 2\text{H}_2\text{O}$, the negative sign of θ is preserved almost within the entire dehydration range, going to positive one, reaching a value of 20 K, and returning back [4]. For $\text{MnC}_2\text{O}_4\cdot 3\text{H}_2\text{O}$ the initial negative θ value changes to positive from the beginning of dehydration and the ferromagnetic interaction is preserved until the beginning of decomposition [4]. For $\gamma\text{-MnC}_2\text{O}_4\cdot 2\text{H}_2\text{O}$ the θ changes its sign twice, but as a whole the trend in the temperature dependence of θ is more similar to that of the monoclinic $\alpha\text{-MnC}_2\text{O}_4\cdot 2\text{H}_2\text{O}$. However, the amplitude in the θ values is highest at $\gamma\text{-MnC}_2\text{O}_4\cdot 2\text{H}_2\text{O}$, which is evidence for much stronger interactions between Mn ions. It can be explained with the structure of $\gamma\text{-MnC}_2\text{O}_4\cdot 2\text{H}_2\text{O}$ in which two adjacent Mn ions are connected via oxygen bridge while in the other two crystal forms the Mn ions are connected via tetradentately coordinated oxalate ion.

The oxidative decomposition takes place above 265 °C and the respective value for the effective magnetic moment is $\mu_{\text{eff}} = 4.6$ BM. It is lower, but relatively close to the value for Mn (III). However, the XRD analysis of the product obtained by isothermal annealing of $\gamma\text{-MnC}_2\text{O}_4\cdot 2\text{H}_2\text{O}$ in air at 300 °C for an hour shows the presence of Mn_3O_4 as a major phase and trace of Mn_5O_8 ($2\text{MnO}\cdot 3\text{MnO}_2$). The theoretical effective magnetic moments of manganese in these oxides are 5.14

BM and 4.43 BM respectively, which means that the value (4.6BM), calculated by us, is determined by the presence of Mn(IV). A further slight increase in the μ_{eff} value to 4.80 BM indicates a secondary reduction process involving CO liberated during decomposition. This reduction of manganese oxidation state explains the increase in the magnetic susceptibility χ_s (Fig. 4a) at the end of the studied temperature range.

The results obtained in the present investigation of $\gamma\text{-MnC}_2\text{O}_4\cdot 2\text{H}_2\text{O}$ can be compared with our results for the other two forms [4]. The μ_{eff} values at 300 °C in the case of initial monoclinic $\alpha\text{-MnC}_2\text{O}_4\cdot 2\text{H}_2\text{O}$, orthorhombic $\gamma\text{-MnC}_2\text{O}_4\cdot 2\text{H}_2\text{O}$ and orthorhombic $\text{MnC}_2\text{O}_4\cdot 3\text{H}_2\text{O}$ are 3.79 BM, 4.80 BM and 4.76 BM. The comparison of the oxidation ability of Mn(II) in different structures reveals similarity between $\gamma\text{-MnC}_2\text{O}_4\cdot 2\text{H}_2\text{O}$ and $\text{MnC}_2\text{O}_4\cdot 3\text{H}_2\text{O}$.

Conclusions. The pinkish $\gamma\text{-MnC}_2\text{O}_4\cdot 2\text{H}_2\text{O}$ was obtained by phase transformation of the initially synthesized $\text{MnC}_2\text{O}_4\cdot 3\text{H}_2\text{O}$ after prolonged residence time in the supernatant liquor. The XRD and SEM analyses confirm the complete transformation of the precursor. The in situ magnetic measurements show that $\gamma\text{-MnC}_2\text{O}_4\cdot 2\text{H}_2\text{O}$ is paramagnetic, similar to the other two forms – $\alpha\text{-MnC}_2\text{O}_4\cdot 2\text{H}_2\text{O}$ and $\text{MnC}_2\text{O}_4\cdot 3\text{H}_2\text{O}$. All of them are antiferromagnetic at room temperature. Based on the changes in the value and sign of Weiss constant with temperature before the decomposition, it could be concluded that the exchange interaction between Mn ions in $\gamma\text{-MnC}_2\text{O}_4\cdot 2\text{H}_2\text{O}$ is stronger than in the other two forms and changes twice from antiferromagnetic to ferromagnetic. The mechanism of decomposition for the three crystal forms $\alpha\text{-MnC}_2\text{O}_4\cdot 2\text{H}_2\text{O}$, $\gamma\text{-MnC}_2\text{O}_4\cdot 2\text{H}_2\text{O}$ and $\text{MnC}_2\text{O}_4\cdot 3\text{H}_2\text{O}$ is the same and proceeds via oxidation of initial Mn(II). However, the oxidation ability of Mn(II) depends on the initial crystal structure of oxalate. It is biggest in monoclinic $\alpha\text{-MnC}_2\text{O}_4\cdot 2\text{H}_2\text{O}$ and similar for both orthorhombic crystal forms $\gamma\text{-MnC}_2\text{O}_4\cdot 2\text{H}_2\text{O}$ and $\text{MnC}_2\text{O}_4\cdot 3\text{H}_2\text{O}$ at the experimental conditions used.

REFERENCES

- [1] DEYRIEUX R., C. BERRO, A. PENELOUX. Bull. Soc. Chim. Fr., **1**, 1973, 25–34.
- [2] LETHBRIDGE Z. A. D., A. F. CONGREVE, E. ESSLEMONT, A. M. Z. SLAWIN, P. LIGHTFOOT. J. Solid State Chem., **172**, 2003, No 1, 212–218.
- [3] WU W.-Y., Y. SONG, Y.-Z. LI, X.-Z. YOU. Inorg. Chem. Commun., **8**, 2005, No 8, 732–736.
- [4] DONKOVA B., D. MEHANDJIEV. Thermochim. Acta, **421**, 2004, Nos 1–2, 141–149.
- [5] JIA Z. G., L. H. YUE, Y. F. ZHENG, Z. D. XU. Chin. J. Inorg. Chem., **23**, 2007, No 1, 181–188.
- [6] DONKOVA B., B. KOTZEVA, D. MEHANDJIEV. Compt. rend. Acad. bulg. Sci., **62**, 2009, No 10, 1229–1234.

- [7] MOHAMED M. A., A. K. GALWEY, S. A. HALAWY. *Thermochimica Acta*, **429**, 2005, No 1, 57–72.
- [8] DOLLIMORE D., D. L. GRIFFITHS. *J. Therm. Anal.*, **2**, 1970, No 3, 229–250.
- [9] MEHANDJIEV D., S. ANGELOV. In: *Magnetochemistry of Solid State*, Sofia, Nauka i izkustvo, 1979, p. 116.
- [10] BOCA R. In: *Theoretical Foundations of Molecular Magnetism*, Oxford, Elsevier Science, 1999, p. 504.

Faculty of Chemistry and Pharmacy
University of Sofia
1, J. Bourchier Blvd
1164 Sofia, Bulgaria
e-mail: nhbd@inorg.chem-uni.sofia.bg

**Institute of Catalysis*
Bulgarian Academy of Sciences
Acad. G. Bonchev Str., Bl. 11
1113 Sofia, Bulgaria